JACS
JOURNAL OF THE AMERICAN CHEMICAL SOCIETY
pubs.acs.org/JACS
Article

Harvesting Water from Air with High-Capacity, Stable Furan-Based Metal−Organic Frameworks

Ali H. Alawadhi, Saumil Chheda, Gautam D. Stroscio, Zichao Rong, Daria Kurandina, Ha L. Nguyen, Nakul Rampal, Zhiling Zheng, Laura Gagliardi,* and Omar M. Yaghi*

Cite This: J. Am. Chem. Soc. 2024, 146, 2160−2166
Read Online

ACCESS | Metrics & More | Article Recommendations | Supporting Information

ABSTRACT: We synthesized two isoreticular furan-based metal−organic frameworks (MOFs), MOF-LA2-1(furan) and MOF-LA2-2(furan) with rod-like secondary building units (SBUs) featuring 1D channels, as sorbents for atmospheric water harvesting (LA = long arm). These aluminum-based MOFs demonstrated a combination of high water uptake and stability, exhibiting working capacities of 0.41 and 0.48 g_{water}/g_{MOF} (under isobaric conditions of 1.70 kPa), respectively. Remarkably, both MOFs showed a negligible loss in water uptake after 165 adsorption−desorption cycles. These working capacities rival that of MOF-LA2-1(pyrazole), which has a working capacity of 0.55 g_{water}/g_{MOF}. The current MOFs stand out for their high water stability, as evidenced by 165 cycles of water uptake and release. MOF-LA2-2(furan) is the first aluminum MOF to employ a double 'long arm' extension strategy, which is confirmed through single-crystal X-ray diffraction (SCXRD). The MOFs were synthesized by using a straightforward synthesis route. This study offers valuable insights into the design of durable, water-stable MOFs and underscores their potential for efficient water harvesting.

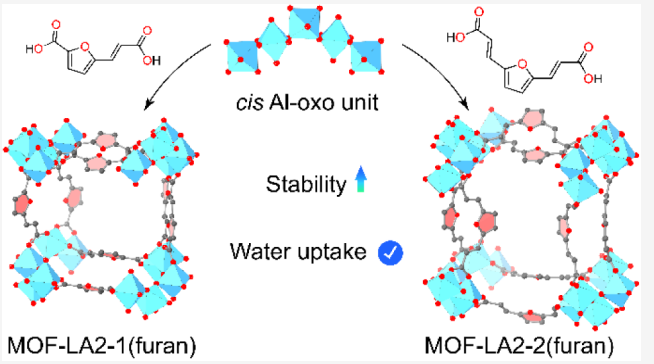

INTRODUCTION

The world is experiencing a water crisis especially in the arid regions, where there are no or limited water resources either above or under the ground.[1−4] Atmospheric water harvesting provides a location-independent solution to global water scarcity.[5,6]

Sorbent-assisted atmospheric water harvesting with metal−organic frameworks (MOFs) is a promising approach.[7−10] This is because MOFs are highly porous, and their structure is tunable.[10−12] These features make MOFs ideal for efficient water harvesting, even under extremely arid conditions.[8,13−15] Atmospheric water harvesting sorbents used in such conditions require a combination of features, including high water uptake, long-term water stability, and fast sorption kinetics.[16]

The use of rod-shaped secondary building units (SBUs) in the design of aluminum MOFs has proven advantageous for water harvesting.[17] This is due to their stability against hydrolysis, and their ability to seed excellent water adsorptive sites within the pores.[8] MOF-303 is an example of an aluminum-based MOF composed of rod-like SBUs, which has been extensively studied for water harvesting.[8,17] A combination of single-crystal X-ray diffraction (SCXRD) and *ab initio* molecular dynamics simulations, reported earlier, has precisely located both the positions at which water adsorbs and the sequence in which the adsorption occurs. Such studies, which provide detailed mechanistic insights into the water adsorption mechanism, can serve as a tool for developing larger pore-sized aluminum MOFs while retaining their unique adsorption properties.

Recently, the 'long arm' (LA) linker extension strategy was employed in synthesizing MOF-LA2-1(pyrazole), an aluminum rod-based MOF that achieved greater water uptake while retaining the favorable properties of its parent, MOF-303.[18] In this study, we report the development of two new MOFs, MOF-LA2-1(furan) and MOF-LA2-2(furan) (Figure 1), and our investigation of their water harvesting performance. We find that these new MOFs are better performing in cyclability and the humidity cutoff, maintaining a high water uptake capacity. We employed SCXRD, powder X-ray diffraction (PXRD), N_2 sorption, H_2O sorption techniques, and density functional theory (DFT) simulations to characterize these new MOFs. MOF-LA2-2(furan) is also the first aluminum MOF to employ a double long arm extension strategy. MOF-LA2-1(furan) and MOF-LA2-2(furan) exhibited step-like water uptakes at 14% and 30% relative humidities (RH), respectively. They also expressed high working capacities of 0.41 g_{water}/g_{MOF} and 0.48

Received: October 26, 2023
Revised: December 27, 2023
Accepted: December 28, 2023
Published: January 11, 2024

https://doi.org/10.1021/jacs.3c11947
J. Am. Chem. Soc. 2024, 146, 2160−2166

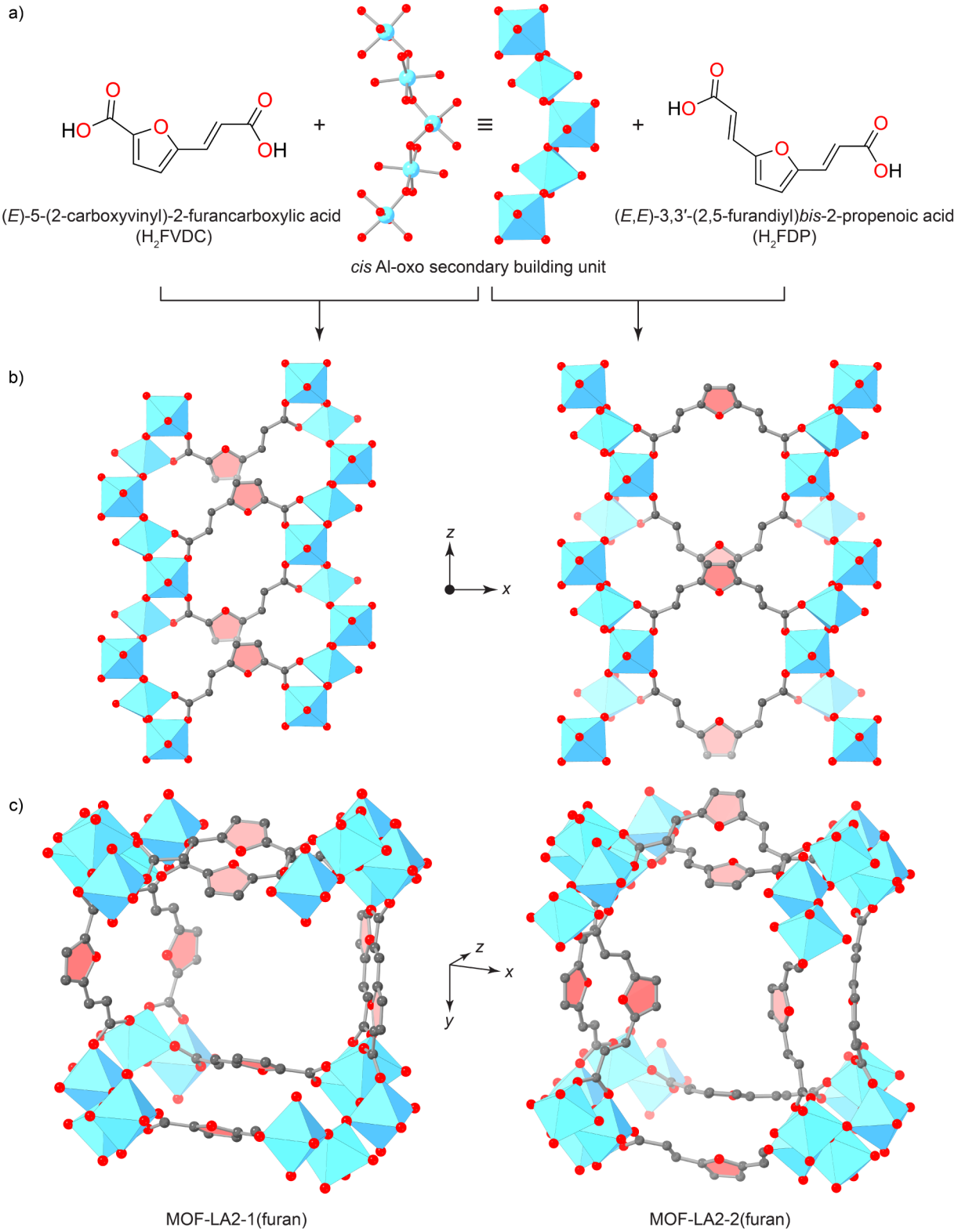

Figure 1. Chemical structures of the H_2FVDC and H_2FDP linkers and the coordinative environment of the *cis* corner-shared SBU (a) from which MOF-LA2-1(furan) (left) and MOF-LA2-2(furan) (right) are constructed. Both MOFs are presented along the *y*-axis perspective (b), expressing the relative conformations of linkers in the framework. They are also presented along the *z*-axis (c) to illustrate a sample of their cuboid 1D channels formed between four sets of *cis* corner-shared SBUs. Polyhedral representation of the aluminum coordination sphere is shown for clarity. Color code: Al, blue octahedron; C, gray; O, red. Hydrogen atoms were omitted for clarity.

g_{water}/g_{MOF} (under isobaric conditions of 1.70 kPa), respectively. Both MOFs demonstrated high durability in water uptake, showing negligible loss in uptake even after more than 165 adsorption−desorption cycles. In the following sections, we detail the synthesis, characterization, and performance evaluation of these MOFs.

https://doi.org/10.1021/jacs.3c11947
J. Am. Chem. Soc. 2024, 146, 2160−2166

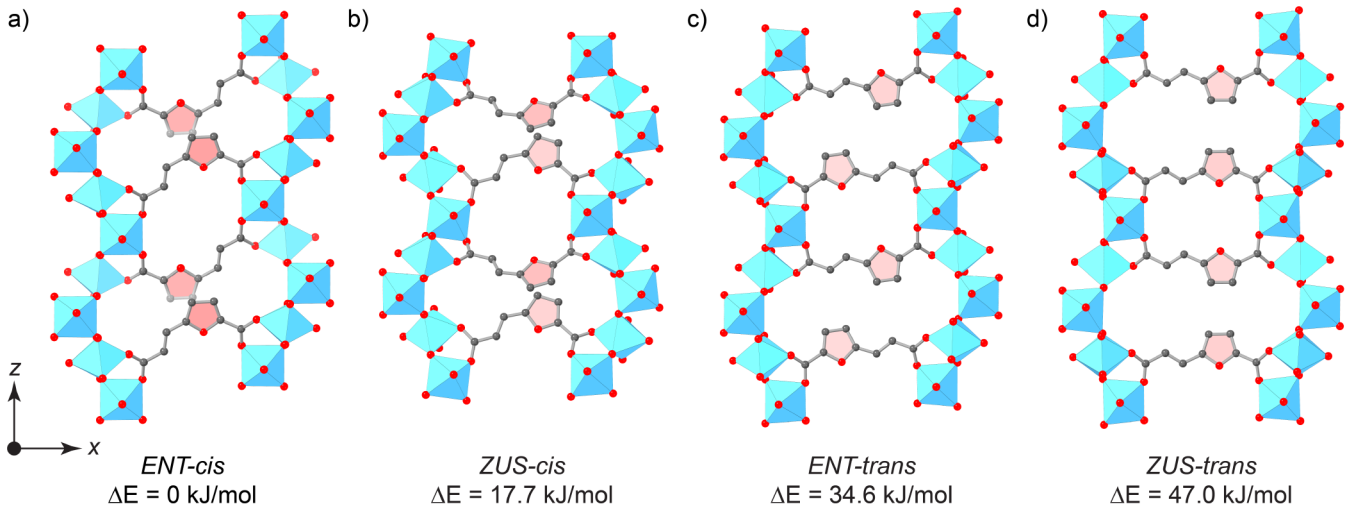

Figure 2. Four theoretical structures of MOF-LA2-1(furan) geometrically optimized using *ab initio* DFT are presented in order of electronic energetic stability per asymmetric unit relative to the most stable *ENT-cis* structure (a) from left to right: *ENT-cis* (a), *ZUS-cis* (b), *ENT-trans* (c), and *ZUS-trans* (d). Labels for each indicate the conformation in which the linker resides in the framework based on the locations of each pair of neighboring linkers relative to each other (*ZUS* or *ENT*) and the relative orientation of the vinyl group to the oxygen heteroatom (*cis* or *trans*). All structures are constructed from a *cis* corner-shared SBU only. Color code: Al, blue octahedron; C, gray; O, red. Hydrogen atoms were omitted for clarity.

RESULTS AND DISCUSSION

Given the moderate water stability reported for MOF-LA2-1(pyrazole), we initially hypothesized that the vinyl group near the *cis*−*trans* corner-shared SBU in this MOF made the Al−$O_{carboxylate}$ bond more susceptible to hydrolysis.[18] This is because vinyl groups in the linker backbone are not bulky enough to provide the steric hindrance required to keep the water molecules away from the Al−$O_{carboxylate}$ bond. To still maintain the advantage of the long arm extension method of higher uptakes, it is, therefore, necessary to either use a bulkier group or use a *cis* corner-shared SBU instead. We used the latter approach because (i) inserting a bulkier group would require a tedious synthesis route, and (ii) it may lead to the reduction of the MOF's pore volume. In addition, *cis* corner-shared SBUs provide more protection due to the shorter distances between subsequent Al atoms (i.e., a more compact structure).

According to previous reports, it has been theorized that the angle formed between the two carboxylic acid groups is what determines the conformation of the corner-shared SBU formed in the structure.[11] We reasoned that using the 2,5-furandicarboxylic acid linker (forms a 130° angle between its two carboxylic acids, as in MIL-160) with the long arm extension strategy would yield a MOF featuring a *cis* corner-shared SBU (Figure 1a).[19,20]

To test our hypothesis, we begin by synthesizing the (*E*)-5-(2-carboxyvinyl)-2-furancarboxylic acid (H_2FVDC) and (*E*,*E*)-3,3′-(2,5-furandiyl)*bis*-2-propenoic acid (H_2FDP) linkers (Figure 1a) using the Doebner-modified Knoevenagel reaction (Sections S1−S3).[21−23] MOF-LA2-1(furan) and MOF-LA2-2(furan) were synthesized with a slight modification of the method used for CAU-10.[19] *N*,*N*-Dimethylformamide (DMF) was selected as a solvent for its dual role: (i) it effectively dissolves the linkers and (ii) acts as a base at elevated temperatures due to its self-decomposition mechanism.[24] The synthesis yielded homogeneous, fine white, and light brown dry powders of MOF-LA2-1(furan) and MOF-LA2-2(furan) (Section S2). It is worth noting that our synthesis conditions were compatible with those used for *cis* corner-shared SBUs containing MOFs like CAU-10 and MIL-160, whereas similar attempts to use synthesis procedures of *cis*−*trans* corner-shared SBUs containing MOFs like MOF-303 and MOF-LA2-1(pyrazole) resulted in noncrystalline materials.[8,15,18,19]

Scanning electron microscopy and energy dispersive X-ray spectroscopy revealed that MOF-LA2-1(furan) formed single crystals approximately 30 μm in size, while MOF-LA2-2(furan) produced single crystals around 100 μm (Section S4). SCXRD analysis performed at the synchrotron yielded a high-resolution diffraction pattern of MOF-LA2-2(furan) compared to MOF-LA2-1(furan); despite multiple attempts to optimize the synthesis conditions of MOF-LA2-1(furan), a resolvable diffraction pattern of the single-crystal could not be obtained. However, as we discuss below, its structure was elucidated by PXRD.

However, MOF-LA2-2(furan) crystallized in a tetragonal $I4_1md$ space group with unit cell parameters of $a = b = 27.0$ Å and $c = 10.6$ Å, and $V = 7754.6$ Å^3 (Section S5). The formula of MOF-LA2-2(furan) was confirmed to be Al(μ_2-OH)(FDP) [corresponding to Al(μ_2-OH)($C_6O_5H_6$)] and in agreement with the aluminum: hydroxyl: linker ratio (1:1:1) known for this class of MOFs that possess rod-like SBUs.[8,15,18,19] The aluminum atoms in MOF-LA2-2(furan) were found to only form a *cis* corner-shared SBU, like that observed in CAU-10 and MIL-160, confirming our hypothesis.[15,19] The distance between sets of four aluminum centers along the same SBU in MOF-LA2-2(furan) was also found to be more compact (10.6 Å) than that in MOF-LA2-1(pyrazole) (12.0 Å).[17] In addition, the observed double bond orientation in the framework results in a more compact arrangement (Figure 1b). The incorporation of vinyl groups in the linkers' backbone offers a 50% increase in pore volume compared to its parent MOF, MIL-160.[15] Overall, MOF-LA2-2(furan) crystallizes forming 1D cuboid shaped channels with a pore size of 11.1 Å (Figure 1c).

Due to the unresolvable SCXRD pattern of MOF-LA2-1(furan) single-crystals, we resorted to constructing different theoretical structures based on *cis* corner-shared SBUs, akin to that observed in the isoreticular MIL-160 and MOF-LA2-2(furan).[15] Here, the conformation of the $FVDC^{2-}$ linker can be described by two main variables. First, the location of two

https://doi.org/10.1021/jacs.3c11947
J. Am. Chem. Soc. 2024, 146, 2160−2166

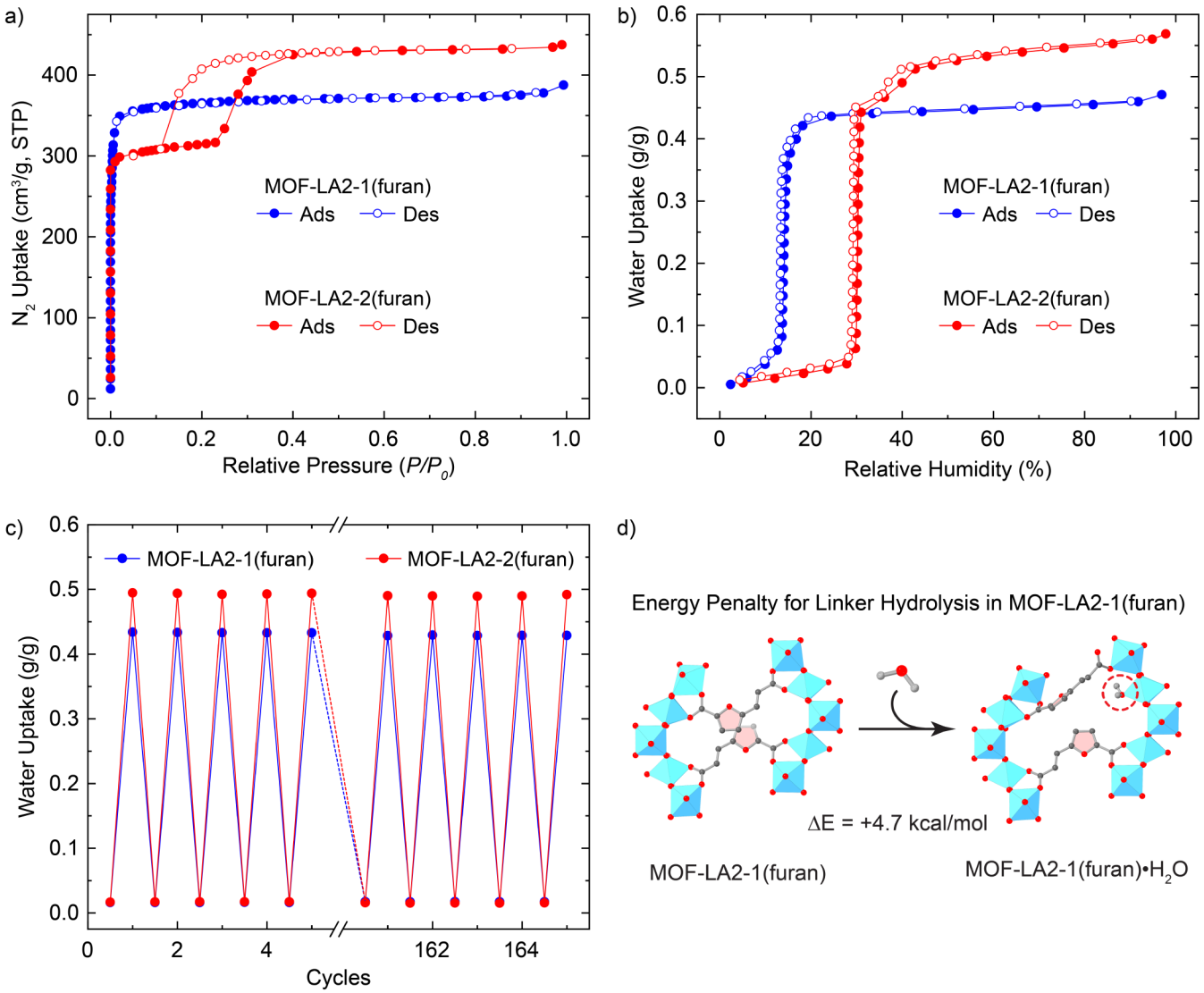

Figure 3. An overview of the major characterization techniques used to compare MOF-LA2-1(furan) (blue) and MOF-LA2-2(furan) (red). (a) Isothermal N_2 sorption plots were measured at 77 K. (b) Isothermal H_2O sorption plots measured at 25 °C. (c) Isobaric H_2O sorption cycling performance was assessed for 165 cycles at a H_2O vapor partial pressure of 1.70 kPa (equivalent to 40% RH at 30 °C). MOF-LA2-1(furan) was cycled between 30 °C (adsorption) and 65 °C (desorption), while MOF-LA2-2(furan) was cycled between 30 °C (adsorption) and 50 °C (desorption). (d) A sample *ab initio* DFT calculation for the hydrolysis of MOF-LA2-1(furan) with the resulting electronic energy penalty presented. The binding of the water molecule to one of the aluminum atoms in the final framework is circled in red. Al, blue octahedron; C, gray; O, red; H in H_2O, white. Hydrogen atoms present in the framework were omitted for clarity.

adjacent furan rings relative to each other, i.e., if they are on the same side with respect to each other (denoted as ZUS from German "zusammen", together) or if they are on opposite sides relative to each other (denoted as ENT from German "entgegen", opposite). Second, the orientation of the vinyl group relative to the heteroatom – here, the vinyl group can be on the same side of the heteroatom (*cis*) or opposite side of it (*trans*). As a result, for MOF-LA2-1(furan), we have the following four possibilities: *ENT-cis*, *ZUS-cis*, *ENT-trans*, and *ZUS-trans* (Figure 2). It is important to reiterate that the corner-shared SBU in all four structures is in a *cis* configuration.

To assess the energetics for these theoretical structures, we optimized their geometry using *ab initio* periodic DFT calculations (Section S6). This allowed us to determine the relative energetic stability of the different structures and thereby identify the thermodynamically most stable structure among them. Out of all the four structures optimized, the *ENT-cis* structure (Figures 1c and 2a) was found to be most stable. This was followed by the *ZUS-cis* (ΔE = 17.7 kJ/mol per asymmetric unit), *ENT-trans* (ΔE = 34.6 kJ/mol), and *ZUS-trans* (ΔE = 47.0 kJ/mol) structures. Generally, the *cis* orientation of the vinyl group relative to the heteroatom was found to be more stable than the *trans* orientation, which is consistent with the energetic stability previously observed in MOF-LA2-1-(pyrazole).[18] The *cis* orientation of the vinyl group is expected to minimize its steric interaction with the aromatic group compared to the *trans* orientation. Furthermore, the *ENT* arrangement of the furan rings was found to be more stable than the *ZUS* arrangement. For the *cis* orientation of the vinyl group, the higher stability of the *ENT* configuration is attributed to possible π-stacking interactions between the furan rings. The *ZUS* arrangement with the *trans* arrangement of the vinyl group, however, is less stable compared to its *ENT* counterpart since the distance between the hydrogen atoms of the opposite-facing

https://doi.org/10.1021/jacs.3c11947
J. Am. Chem. Soc. 2024, 146, 2160−2166

vinyl group in this arrangement is less than the sum of their van der Waal's radii ($r_{vdW,\ hydrogen}$ = 1.2 Å). Henceforth, all values calculated for the MOF LA2-1(furan) correspond to those obtained for the *ENT-cis* structure.

PXRD analysis of MOF-LA2-1(furan) revealed high crystallinity, as evidenced by a full width at half-maximum (fwhm) of 0.10° for the peak at $2\theta = 7.63°$ (Section S7). Pawley refinement of the structure against the experimental PXRD resulted in low reliability factors. The final cell parameters of MOF-LA2-1(furan) structure forming a tetragonal $I4_1/a$ space group were with final cell parameters of $a = b = 24.0$ Å and $c = 10.5$ Å. These parameters agree with the results obtained from *ab initio* DFT calculations, in which the *ENT-cis* structure was determined to be the most energetically stable structure. The MOF-LA2-1(furan) structure was, therefore, confirmed to be isoreticular to the MOF-LA2-2(furan), forming with a *cis* corner-shared SBU and having a pore size of 9.2 Å with 1D cuboid channels.

We also performed PXRD analysis on the MOF-LA2-2(furan) sample to confirm that the bulk powder phase was consistent with the SCXRD-obtained crystal structure (Section S7). The resulting PXRD pattern indicated a highly crystalline bulk powder, as evidenced by a fwhm of 0.10° at the $2\theta = 6.51°$ peak. The pattern also matched the simulated pattern generated from the obtained single-crystal structure.

Next to assess the pore volume and Brunauer−Emmett−Teller (BET) area for both MOF-LA2-1(furan) and MOF-LA2-2(furan), we conducted N_2 sorption measurements at 77 K (Figure 3a).[25] The BET areas were determined to be 1113 m^2/g for MOF-LA2-1(furan) and 1269 m^2/g for MOF-LA2−2(furan) (Section S8). Their theoretical surface areas, calculated using the BIOVIA Materials Studio 2020 software, are 1209 m^2/g and 1550 m^2/g, respectively. These theoretical values were calculated based on the DFT-optimized structure for MOF-LA2-1(furan) and the single-crystal structure data for MOF-LA2-2(furan).

We found that the experimentally determined pore volumes exceeded the theoretical estimates. Experimental pore volumes were 0.586 cm^3/g and 0.673 cm^3/g, assuming micropore filling only for $P/P_0 < 0.95$, calculated using Gurvich rule.[26] These values surpass the theoretical pore volumes of 0.433 cm^3/g for MOF-LA2-1(furan) and 0.597 cm^3/g for MOF-LA2-2(furan) calculated by considering a Connolly surface using a probe of diameter 3.64 Å corresponding to N_2.[27]

Discrepancies in the pore volume of both MOFs prompted a closer examination of the N_2 sorption isotherms. When MOF-LA2-1(furan) was analyzed using a logarithmic-scaled partial pressure, both MOF-LA2-1(furan) and MOF-LA2-2(furan) exhibited a two-step N_2 uptake (Section S8). Notably, the pore volumes corresponding to the first step of N_2 uptake in both isotherms closely matched the theoretical pore volumes previously determined. This suggests that the crystal structures are representative only at low partial pressures − specifically, at $P/P_0 < 0.0032$ for MOF-LA2-1(furan) and $P/P_0 < 0.23$ for MOF-LA2-2(furan) (P_0 = 1 atm), where the BET areas were calculated based on the first step for each of the two MOFs. We hypothesize that the second step in the N_2 sorption isotherms may involve a form of reversible pore expansion. Attempts to isolate and characterize the expanded form of MOF-LA2-2(furan) were thus far proved unsuccessful; further studies in this regard are ongoing.

Encouraged by the high surface area and pore volume of the MOFs, we subjected them to a water sorption analysis. Water sorption profiles were measured for both MOFs at three different temperatures: 25 °C, 35 °C, and 45 °C (Section S9). For MOF-LA2-1(furan), a sharp, step-like isotherm was observed at 14% RH, with a total water uptake of 0.47 g_{water}/g_{MOF} under 25 °C conditions (Figure 3b). MOF-LA2-2(furan) exhibited a similar step-like isotherm but at 30% RH, and its total water uptake was 0.57 g_{water}/g_{MOF} at 25 °C (Figure 3b). Additionally, the average isosteric heats of adsorption (Q_{st}) for water calculated using the Clausius−Clapeyron relation are 53 kJ/mol for MOF-LA2-1(furan) and 50 kJ/mol for MOF-LA2-2(furan) (Section S9), which are comparable to that of MOF-LA2-1(pyrazole) (51 kJ/mol).[18,28,29]

Having characterized the crystallinity and porosity of both MOFs, next we conducted cycling experiments to evaluate the long-term water sorption performance (Figure 3c). First, to determine the optimal water desorption temperatures at isobaric conditions (1.70 kPa, equivalent to 40% RH at 30 °C) for both MOFs, we performed isobaric water sorption measurements (Section S9). Based on isobaric desorption water measurements, 65 and 50 °C were identified as suitable desorption temperatures for MOF-LA2-1(furan) and MOF-LA2-2(furan) at a partial pressure of 1.70 kPa, respectively. For MOF-LA2-1(furan), approximately 0.41 g_{water}/g_{MOF} could be adsorbed and desorbed within a temperature range of 30−65 °C. This represents 87% of the MOF's total possible water uptake capacity under these conditions. Similarly, MOF-LA2-2(furan) could desorb 0.48 g_{water}/g_{MOF} within a temperature range of 30−50 °C, accounting for 84% of its maximum water uptake capacity. Subsequently, we performed 165 adsorption−desorption cycles for MOF-LA2-1(furan), which exhibited a negligible decrease in water uptake capacity (1%). MOF-LA2-2(furan) retained its water uptake capacity after 165 adsorption−desorption cycles (Section S9). In comparison, MOF-LA2-1(pyrazole) exhibited a 6% drop in water uptake after 150 cycles.[18]

The significant differences observed in the long term water stability between these MOFs and MOF-LA2-1(pyrazole) led us to further investigate its origins. Our hypothesis centers on the role of *cis* corner-shared SBU arrangement in these long-arm-based MOFs, in maintaining the stability of Al−$O_{carboxylate}$ bonds.

To test this hypothesis, we employed *ab initio* cluster-DFT calculations (Section S6). We created representative truncated cluster models for four different MOFs: MOF-303, MOF-LA2-1(pyrazole), MIL-160, and the newly reported MOF-LA2-1(furan) by extracting relevant portions from their original structures.[15,18]

We calculated the electronic energy change associated with the hydrolysis of one Al−$O_{carboxylate}$ linkage, where the coordinating oxygen atom (from a carboxylate group) was substituted with a water molecule. The linker hydrolysis penalty for the pyrazole-based MOFs was found to decrease from 8.4 kcal/mol [MOF-303] to 2.8 kcal/mol [MOF-LA2-1(pyrazole)] upon the addition of the "long arm" extension ($\Delta\Delta E = -5.6$ kcal/mol), while the energy penalty was found to only decrease from 5.3 kcal/mol [MIL-160] to 3.4 kcal/mol [MOF-LA2-1(furan)] for the furan-based MOFs ($\Delta\Delta E = -1.9$ kcal/mol), suggesting that the furan-based MOFs (bearing *cis*-only rod SBUs) retain the high hydrolytic stability of the parent MOF upon addition of long-arm substituent compared to the pyrazole-based MOFs (bearing *cis*−*trans* rod SBUs). The smaller change in the linker hydrolysis penalty for the furan-based MOFs can be attributed to the lower accessibility of the Al centers by a water molecule in these MOFs as evinced by the shorter distance between sets of four aluminum atoms in the

https://doi.org/10.1021/jacs.3c11947
J. Am. Chem. Soc. 2024, 146, 2160−2166

MOFs bearing *cis*-only rod SBUs (10.3 Å) compared to the MOF bearing the *cis*−*trans* rod SBU (12.0 Å). These differing energies underscore a significant variation in the required energy penalty for hydrolyzing the MOFs. Thus, we attribute the chemical robustness and hydrolytic stability of these MOFs to the extra energy penalty required for linker dissociation.

CONCLUSION

In conclusion, we successfully synthesized two new MOFs, MOF-LA2-1(furan) and MOF-LA2-2(furan), designed for enhanced water harvesting. MOF-LA2-2(furan) was specifically characterized using SCXRD. Both MOFs synthesized provided high working capacities of 0.41 g_{water}/g_{MOF} and 0.48 g_{water}/g_{MOF}, while having negligible losses in uptake even after more than 165 water adsorption−desorption cycles. The origins of this enhanced stability were also studied by using *ab initio* DFT calculations.

ASSOCIATED CONTENT

Supporting Information

The Supporting Information is available free of charge at https://pubs.acs.org/doi/10.1021/jacs.3c11947.

Synthesis and full characterization of MOFs including NMR spectroscopy, EA, computational studies, SCXRD data, PXRD data, N_2 sorption data, H_2O sorption data, SEM and EDS images (PDF)

Accession Codes

CCDC 2303711 contains the supplementary crystallographic data for this paper. These data can be obtained free of charge via www.ccdc.cam.ac.uk/data_request/cif, or by emailing data_request@ccdc.cam.ac.uk, or by contacting The Cambridge Crystallographic Data Centre, 12 Union Road, Cambridge CB2 1EZ, UK; fax: +44 1223 336033.

AUTHOR INFORMATION

Corresponding Authors

Laura Gagliardi − *Department of Chemistry, Pritzker School of Molecular Engineering, and Chicago Center for Theoretical Chemistry, University of Chicago, Chicago, Illinois 60637, United States;* orcid.org/0000-0001-5227-1396; Email: lgagliardi@uchicago.edu

Omar M. Yaghi − *Department of Chemistry, University of California, Berkeley, California 94720, United States; Kavli Energy Nanoscience Institute and Bakar Institute of Digital Materials for the Planet, College of Computing, Data Science, and Society, University of California, Berkeley, California 94720, United States; KACST−UC Berkeley Center of Excellence for Nanomaterials for Clean Energy Applications, King Abdulaziz City for Science and Technology, Riyadh 11442, Saudi Arabia;* orcid.org/0000-0002-5611-3325; Email: yaghi@berkeley.edu

Authors

Ali H. Alawadhi − *Department of Chemistry, University of California, Berkeley, California 94720, United States; Kavli Energy Nanoscience Institute and Bakar Institute of Digital Materials for the Planet, College of Computing, Data Science, and Society, University of California, Berkeley, California 94720, United States;* orcid.org/0000-0003-2680-5221

Saumil Chheda − *Department of Chemical Engineering and Materials Science, Department of Chemistry and Chemical Theory Center, University of Minnesota−Twin Cities, Minneapolis, Minnesota 55455, United States;* Present Address: Department of Chemistry, Kavli Energy Nanoscience Institute, and Bakar Institute of Digital Materials for the Planet, College of Computing, Data Science, and Society, University of California, Berkeley, California 94720, United States; orcid.org/0000-0002-0989-5707

Gautam D. Stroscio − *Department of Chemistry, Pritzker School of Molecular Engineering, and Chicago Center for Theoretical Chemistry, University of Chicago, Chicago, Illinois 60637, United States;* orcid.org/0000-0002-0827-1062

Zichao Rong − *Department of Chemistry, University of California, Berkeley, California 94720, United States; Kavli Energy Nanoscience Institute and Bakar Institute of Digital Materials for the Planet, College of Computing, Data Science, and Society, University of California, Berkeley, California 94720, United States;* orcid.org/0000-0002-9014-9540

Daria Kurandina − *Department of Chemistry, University of California, Berkeley, California 94720, United States; Kavli Energy Nanoscience Institute and Bakar Institute of Digital Materials for the Planet, College of Computing, Data Science, and Society, University of California, Berkeley, California 94720, United States;* Present Address: Seagen, 21823 30th Dr SE, Bothell, Washington 98021, United States

Ha L. Nguyen − *Department of Chemistry, University of California, Berkeley, California 94720, United States; Kavli Energy Nanoscience Institute and Bakar Institute of Digital Materials for the Planet, College of Computing, Data Science, and Society, University of California, Berkeley, California 94720, United States;* orcid.org/0000-0002-4977-925X

Nakul Rampal − *Department of Chemistry, University of California, Berkeley, California 94720, United States; Kavli Energy Nanoscience Institute and Bakar Institute of Digital Materials for the Planet, College of Computing, Data Science, and Society, University of California, Berkeley, California 94720, United States*

Zhiling Zheng − *Department of Chemistry, University of California, Berkeley, California 94720, United States; Kavli Energy Nanoscience Institute and Bakar Institute of Digital Materials for the Planet, College of Computing, Data Science, and Society, University of California, Berkeley, California 94720, United States;* orcid.org/0000-0001-6090-2258

Complete contact information is available at: https://pubs.acs.org/10.1021/jacs.3c11947

Notes

The authors declare the following competing financial interest(s): O.M.Y. is cofounder of Water Harvesting Inc. and ATOCO Inc., aiming at commercializing related technologies. This work has been filed as US Provisional Patent Application No. 63/342,060.

ACKNOWLEDGMENTS

We acknowledge financial support from the Defense Advanced Research Projects Agency (DARPA) under contract HR0011-21-C-0020. Any opinions, findings, and conclusions or recommendations expressed in this material are those of the author(s) and do not necessarily reflect the views of DARPA. This research used resources of the Advanced Light Source, which is a DOE Office of Science User Facility under contract No. DE-AC02-05CH11231. S.C. acknowledges the financial support from the Department of Energy, Office of Basic Energy

Sciences, Division of Chemical Sciences, Geosciences and Biosciences under Award DE-FG02-17ER16362. G.D.S. and L.G. were partially supported by NSF, Division of Chemistry, Chemical Structure, Dynamics, and Mechanisms A (CSDM-A) Award Number: CHE-2223442. The authors are thankful to the Research Computing Center at the University of Chicago to provide the computational resources for this work. We thank Dr. Hasan Celik of UC Berkeley's NMR facility in the College of Chemistry for spectroscopic assistance. The NMR facility in the College of Chemistry at UC Berkeley is supported in part by NIH S10OD024998. We thank the Molecular Graphics and Computation Facility in the College of Chemistry at UC Berkeley, which is supported by NIH S10OD034382. We would like to thank Dr. Nikita Hanikel (Yaghi Group, UC Berkeley) and Dr. David Moore (General Electric) for their helpful comments and discussions. We also would like to thank Ephraim Neumann (Yaghi Group, UC Berkeley) for his assistance in scanning-electron microscopy measurements.

REFERENCES

(1) Mekonnen, M. M.; Hoekstra, A. Y. Four Billion People Facing Severe Water Scarcity. *Sci. Adv.* **2016**, *2* (2), No. e1500323.
(2) van Vliet, M. T. H.; Jones, E. R.; Flörke, M.; Franssen, W. H. P.; Hanasaki, N.; Wada, Y.; Yearsley, J. R. Global Water Scarcity Including Surface Water Quality and Expansions of Clean Water Technologies. *Environ. Res. Lett.* **2021**, *16*, 024020.
(3) Hoekstra, A. Y.; Mekonnen, M. M. The Water Footprint of Humanity. *Proc. Natl. Acad. Sci. U. S. A.* **2012**, *109* (9), 3232−3237.
(4) Famiglietti, J. S. The Global Groundwater Crisis. *Nat. Clim. Change* **2014**, *4*, 945−948.
(5) Lu, H.; Shi, W.; Guo, Y.; Guan, W.; Lei, C.; Yu, G. Materials Engineering for Atmospheric Water Harvesting: Progress and Perspectives. *Adv. Mater.* **2022**, *34* (12), 2110079.
(6) Peeters, R.; Vanderschaeghe, H.; Rongé, J.; Martens, J. A. Energy Performance and Climate Dependency of Technologies for Fresh Water Production from Atmospheric Water Vapour. *Environ. Sci.: Water Res. Technol.* **2020**, *6*, 2016−2034.
(7) Furukawa, H.; Gándara, F.; Zhang, Y.-B.; Jiang, J.; Queen, W. L.; Hudson, M. R.; Yaghi, O. M. Water Adsorption in Porous Metal-Organic Frameworks and Related Materials. *J. Am. Chem. Soc.* **2014**, *136* (11), 4369−4381.
(8) Fathieh, F.; Kalmutzki, M. J.; Kapustin, E. A.; Waller, P. J.; Yang, J.; Yaghi, O. M. Practical Water Production from Desert Air. *Sci. Adv.* **2018**, *4* (6), No. eaat3198.
(9) Furukawa, H.; Cordova, K. E.; O'Keeffe, M.; Yaghi, O. M. The Chemistry and Applications of Metal-Organic Frameworks. *Science* **2013**, *341* (6149), 1230444.
(10) Yaghi, O. M.; O'Keeffe, M.; Ockwig, N. W.; Chae, H. K.; Eddaoudi, M.; Kim, J. Reticular Synthesis and the Design of New Materials. *Nature* **2003**, *423*, 705−714.
(11) Zheng, Z.; Hanikel, N.; Lyu, H.; Yaghi, O. M. Broadly Tunable Atmospheric Water Harvesting in Multivariate Metal-Organic Frameworks. *J. Am. Chem. Soc.* **2022**, *144* (49), 22669−22675.
(12) Eddaoudi, M.; Kim, J.; Rosi, N.; Vodak, D.; Wachter, J.; O'Keeffe, M.; Yaghi, O. M. Systematic Design of Pore Size and Functionality in Isoreticular MOFs and Their Application in Methane Storage. *Science* **2002**, *295* (5554), 469−472.
(13) Hanikel, N.; Prévot, M. S.; Fathieh, F.; Kapustin, E. A.; Lyu, H.; Wang, H.; Diercks, N. J.; Glover, T. G.; Yaghi, O. M. Rapid Cycling and Exceptional Yield in a Metal-Organic Framework Water Harvester. *ACS Cent. Sci.* **2019**, *5* (10), 1699−1706.
(14) Song, W.; Zheng, Z.; Alawadhi, A. H.; Yaghi, O. M. MOF Water Harvester Produces Water from Death Valley Desert Air in Ambient Sunlight. *Nat. Water* **2023**, *1*, 626−634.
(15) Cadiau, A.; Lee, J. S.; Damasceno Borges, D.; Fabry, P.; Devic, T.; Wharmby, M. T.; Martineau, C.; Foucher, D.; Taulelle, F.; Jun, C. H.; Hwang, Y. K.; Stock, N.; De Lange, M. F.; Kapteijn, F.; Gascon, J.; Maurin, G.; Chang, J. S.; Serre, C. Design of Hydrophilic Metal Organic Framework Water Adsorbents for Heat Reallocation. *Adv. Mater.* **2015**, *27* (32), 4775−4780.
(16) Yang, P.; Clark, D. S.; Yaghi, O. M. Envisioning the "Air Economy" — Powered by Reticular Chemistry and Sunlight for Clean Air, Clean Energy, and Clean Water. *Mol. Front. J.* **2021**, *05* (01n02), 30−37.
(17) Hanikel, N.; Pei, X.; Chheda, S.; Lyu, H.; Jeong, W. S.; Sauer, J.; Gagliardi, L.; Yaghi, O. M. Evolution of Water Structures in Metal-Organic Frameworks for Improved Atmospheric Water Harvesting. *Science* **2021**, *374* (6566), 454−459.
(18) Hanikel, N.; Kurandina, D.; Chheda, S.; Zheng, Z.; Rong, Z.; Neumann, S. E.; Sauer, J.; Siepmann, J. I.; Gagliardi, L.; Yaghi, O. M. MOF Linker Extension Strategy for Enhanced Atmospheric Water Harvesting. *ACS Cent. Sci.* **2023**, *9* (3), 551−557.
(19) Reinsch, H.; van der Veen, M. A.; Gil, B.; Marszalek, B.; Verbiest, T.; de Vos, D.; Stock, N. Structures, Sorption Characteristics, and Nonlinear Optical Properties of a New Series of Highly Stable Aluminum MOFs. *Chem. Mater.* **2013**, *25* (1), 17−26.
(20) Guo, L.; Hurd, J.; He, M.; Lu, W.; Li, J.; Crawshaw, D.; Fan, M.; Sapchenko, S.; Chen, Y.; Zeng, X.; Kippax-Jones, M.; Huang, W.; Zhu, Z.; Manuel, P.; Frogley, M. D.; Lee, D.; Schröder, M.; Yang, S. Efficient Capture and Storage of Ammonia in Robust Aluminium-Based Metal-Organic Frameworks. *Commun. Chem.* **2023**, *6*, 55.
(21) Sibi, M. P.; Sermadurai, S.; Zimmermann, N.; Serum, E.; Ma, G.; Moorthy, R.; Kalliokoski, K. Novel Monomers From Biomass. WO 2,016,022,943 A2, 2016.
(22) Doebner, O. Ueber Die Der Sorbinsäure Homologen, Ungesättigten Säuren Mit Zwei Doppelbindungen. *Ber. Dtsch. Chem. Ges.* **1902**, *35* (1), 1136−1147.
(23) Knoevenagel, E. Condensation von Malonsäure Mit Aromatischen Aldehyden Durch Ammoniak Und Amine. *Ber. Dtsch. Chem. Ges.* **1898**, *31* (3), 2596−2619.
(24) Yaghi, O. M.; Kalmutzki, M. J.; Diercks, C. S. *Introduction to Reticular Chemistry: Metal-Organic Frameworks and Covalent Organic Frameworks*; Wiley-VCH: Weinheim, 2019. DOI: DOI: 10.1002/9783527821099.
(25) Brunauer, S.; Emmett, P. H.; Teller, E. Adsorption of Gases in Multimolecular Layers. *J. Am. Chem. Soc.* **1938**, *60* (2), 309−319.
(26) Gurvich, L. *J. Phys. Chem. Soc. Russ.* **1915**, *47*, 49−56.
(27) Connolly, M. L. Computation of Molecular Volume. *J. Am. Chem. Soc.* **1985**, *107* (5), 1118−1124.
(28) Clausius, R. Ueber Die Bewegende Kraft Der Wärme Und Die Gesetze, Welche Sich Daraus Für Die Wärmelehre Selbst Ableiten Lassen. *Ann. Phys.* **1850**, *155* (3), 368−397.
(29) Clapeyron, B. P. É Mémoire Sur La Puissance Motrice de La Chaleur. *Journal. de. l'Ecole. Polytechnique* **1834**, *14*, 23.

https://doi.org/10.1021/jacs.3c11947
J. Am. Chem. Soc. 2024, 146, 2160−2166